Environ Geochem Health (2018) 40:1979–1986
https://doi.org/10.1007/s10653-017-0001-z

ORIGINAL PAPER

Study of the interactions of dissolved organic matter with zinc ion and the impact of competitive metal ions (Ca^{2+} and Mg^{2+}) by in situ absorbance

Tianyu Zhang · Tao Wang · Yujuan Lu

Received: 18 January 2017 / Accepted: 12 June 2017 / Published online: 22 June 2017

Abstract The bioavailability and toxicity of zinc to aquatic life depend on dissolved organic matter (DOM), such as Suwannee River Fulvic Acid (SRFA), which plays an important role in the speciation of zinc. This study examined reactions of SRFA with zinc at different concentrations from pH 3.0 to 9.0, and competitive binding of calcium/magnesium and zinc to SRFA at pH 6.0, using in situ absorbance. Interactions of Zn^{2+} with SRFA chromophores were evidenced by the emergence of features in Zn-differential spectra. Among all Zn^{2+}–SRFA systems, dominant peaks, located at 235, 275 and 385 nm, and the highest intensity at 235 nm indicated the replacement of protons by the bound Zn^{2+}. The Zn^{2+} binding with SRFA could be quantified by calculating the changes of the slopes of Zn-differential log-transformed absorbance in the wavelength range of 350–400 nm (denoted as $DS_{350–400}$) and by comparing the experimental data with predictions using the Non-Ideal Competitive Adsorption (NICA–Donnan) model. $DS_{350–400}$ was correlated well with the bound Zn^{2+} concentrations predicted by NICA–Donnan model with or without Ca^{2+} or Mg^{2+}. Ca^{2+} and Mg^{2+} only affect intensity of the Zn-differential and Zn-differential log-transformed absorbance, not shape. In situ absorbance can be used to gain further information about Me^{n+}–DOM interactions in the presence of various metals.

Keywords Zinc ion · Dissolved organic matter · In situ methods of absorbance · NICA–Donnan model

Introduction

Dissolved organic matter (DOM) affects the speciation of zinc in natural waters (Mueller et al. 2012) and plays an important role in protecting aquatic organisms against toxicity of excessive zinc (Heijerick and Janssen 2000, Schamphelaere et al. 2005). The composition of DOM relies on sources of organic matter, ionic strength, pH and major cation in water (Leenheer and Croué 2003). Current techniques for quantifying DOM–metals interactions are very diverse, such as ion exchange technique (IET) (Fortin et al. 2010), ion-selective electrodes (ISEs) (Valilue

Electronic supplementary material The online version of this article (doi:10.1007/s10653-017-0001-z) contains supplementary material, which is available to authorized users.

T. Wang · Y. Lu (✉)
College of Chemistry and Environmental Engineering, Shenzhen University, Shenzhen 518060, Guangdong, People's Republic of China
e-mail: yjlv@szu.edu.cn

T. Zhang
Department of Mathematical Economics and Mathematical Finance, Economics and Management School of Wuhan University, Wuhan, People's Republic of China

et al. 2016), cathodic stripping voltammetry (Wasag and Grabarczyk 2016) and Donnan membrane technique (Jones et al. 2016). Although these methods have been used to determine free metal ion concentrations in natural waters, the performance of many assays remains inadequate for the complexity of analytical matrices and very low ambient metal concentrations.

Absorbance spectroscopy has been used widely to test the reactivity between DOM and free metal ions. It was proved to be high sensitive to the variation of the composition of DOM and could track trace metal ion concentrations without any sample pre-concentration (Yan et al. 2013; Gao et al. 2015a, b). However, the absorbance spectroscopy of DOM–metals is featureless. An alternative in situ method, differential absorbance spectroscopy (DAS) (Dryer et al. 2008), was proved to be useful for revealing interpretable features associated with deprotonation of DOM molecules and the reaction with metal ions. In addition, Windermere Humic Aqueous Model (WHAM) and the Non-Ideal Competitive Adsorption (NICA)–Donnan model can predict *concentrations of free metal ions to DOM binding* in natural waters (Dudal and Gérard 2004).

In this study, we used in situ absorbance spectroscopy to track interactions between DOM and Zn^{2+} per se at a wide range of pHs, as well as Zn^{2+} in the presence of different concentrations of Ca^{2+}/Mg^{2+} at pH 6.0. These background ions affect various heavy metals binding on SRFA. The spectroscopic data were processed and compared with the predicted data of NICA–Donnan model, which allowed the quantitation of metal binding on SRFA.

Materials and methods

Reagents and chemicals

All chemicals used are reagent grade, unless mentioned specifically. All solutions were prepared using Milli-Q water (18.2 MΩ cm^{-1}, Millipore Corp., MA, USA). Suwannee River Fulvic Acid (SRFA) (standard number 1S101F) was acquired from the International Humic Substances Society (IHSS). SRFA is deemed to be representative of a wide range of DOM types in the environment (Maurice 2015). The dissolved organic carbon (DOC) concentration of SRFA was 5.0 mg L^{-1} as DOC. The concentrations of residual metal cations in the SRFA sample were negligible (Kuhn et al. 2015). Ionic strength of SRFA solutions (0.01 mol L^{-1}) was regulated by adding $NaClO_4$ background electrolyte. Stock solutions (Zn^{2+}, Ca^{2+} and Mg^{2+}) were prepared using $ZnCl_2$, $CaCl_2{\cdot}2H_2O$ and $MgCl_2{\cdot}6H_2O$ salts from Aladdin reagent Shanghai Co. Ltd. (Aldrich Chemical Company, Shanghai, China).

Titrations

We conducted Zn^{2+} titrations according to the procedures for different metal ions previously described (Yan and Korshin 2004; Yan et al. 2013, 2015; Gao et al. 2015a, b). A certain amount of Zn^{2+} stock solution was added into a series of 40 mL-jars SRFA at pH 5.0–9.0, and a series of 40 mL-jars SRFA with or without 0.00025 and 0.0025 mol L^{-1} Ca^{2+} or 0.0004 and 0.004 mol L^{-1} Mg^{2+} at ionic strength 0.01 mol L^{-1}, pH 6.0.

Total Zn^{2+} concentrations were varied from 0 to 10^{-6} mol L^{-1}, which was below its precipitation level determined using Visual MINTEQ. We analyzed SRFA–metal complexation using the NICA–Donnan model (Benedetti et al. 1996; Kinniburgh et al. 1999; Milne et al. 2003). Complexation constants from Visual MINTEQ database used in the calculations are marked in Table S1. We adjusted the pH of the solutions by adding small amounts of $HClO_4$ or NaOH. Also, we added 0.01 mol L^{-1} MES buffer to the solutions with low buffering capacity (e.g., at pH 6.0). This buffer does not affect the ionic strength of SRFA solutions or absorbing light above ca. 230 nm (And and Rorabacher 1999). After adding metal stock solution, followed by mixing and standing for 30 min, absorbance spectra of aliquots from solutions with various metal concentrations were conducted on a Perkin-Elmer Lambda 2550 UV–Vis spectrophotometer with a 5-cm cell at wavelengths from 200 to 800 nm.

Absorbance data processing

Data processing of SRFA absorbance spectra was done as described in previous studies (Yan and Korshin 2004; Yan et al. 2013, 2016; Gao et al. 2015a, b). The differential linear spectra and differential log-transformed spectra were calculated using

Eqs. (1), (2), respectively (Dryer et al. 2008; Gao et al. 2015a, b):

$$\mathrm{DA}_{\lambda} = \frac{1}{\mathrm{DOC} \cdot L}\left[A_{\lambda,i} - A_{\lambda,\mathrm{ref}}\right] \quad (1)$$

$$\mathrm{DLnA}_{\lambda} = \mathrm{LnA}_{\lambda,i} - \mathrm{LnA}_{\lambda,\mathrm{ref}} \quad (2)$$

In these formulas, $A_{\lambda,i}$ is DOM absorbance measured at the wavelength λ for any selected condition (i), and $A_{\lambda,\mathrm{ref}}$ is DOM absorbance measured at the wavelength λ for an applicable reference (ref, e.g., zero total metal or zinc concentration, DOC is the concentration of organic carbon (mg/L), and length is the cell length (in cm). The slopes and differential slopes of log-transformed absorbance spectra of DOM were calculated as follows:

$$S_{350-400} = \left|\frac{d\ln A(\lambda)}{d\lambda}\right|_{350-400} \quad (3)$$

$$\mathrm{DS}_{350-400} = S_{350-400,i} - S_{350-400,\mathrm{ref}}. \quad (4)$$

In the above equations, $S_{350–400}$ is the slope of the linear correlation that fit the log-transformed DOM absorbance spectra in the range between 350 and 400 nm. $S_{350–400,\mathrm{i}}$ and $S_{350–400,\mathrm{ref}}$ are the spectral slopes determined for any selected experimental condition and applicable reference (ref, e.g., zero total metal or zinc concentration), respectively. The prefix D denotes the differential between any selected experimental condition and the applicable reference against which that differential is calculated.

Results and discussion

Effect of Zn^{2+} binding on SRFA chromophores

As illustrated in Fig. 1a for SRFA at pH 9.0 and ionic strength 0.01 mol L^{-1}, the zero-order absorbance spectra of SRFA have no conspicuous features and the intensity of them decreases near exponentially with the observation wavelength. By increasing zinc concentration, subtle but consistent changes in zero-order absorbance spectra were detected, which was consistent with previous studies of metal–SRFA interactions (Yan and Korshin 2004; Yan et al. 2013; Gao et al. 2015a, b). To gain more information of the interactions of Zn^{2+}–SRFA, we calculated DOC-normalized differential spectra (DAS) using Eq. 1, presented in Fig. 1b. Three distinct bands with peaks at ca. 235, 275 and 385 nm were identified, and the strongest was at ca. 235 nm. The shape change of absorbance spectra was stable when zinc concentration increased. As previously described (Dryer et al. 2008), the band at ca. 280 nm was likely associated with the deprotonation of carboxylic groups in SRFA, while the bands at ca. 244 nm and in the 300–390 nm region reflected the deprotonation of phenolic group in SRFA.

Figure 1c demonstrates that the logarithms of absorbance of Zn^{2+}–SRFA decreased linearly with the wavelength. However, the log-transformed spectra were made of several regions (e.g., <250, 250–400 and >400 nm) with slightly different slopes.

Figure 1d shows that the slopes of the log-transformed spectra have consistent changes at various zinc concentrations, and the slope of log-transformed absorbance of SRFA in wavelengths 350–400 nm would be the most sensitive range to the change of Zn^{2+} concentrations. Thence, the absolute slope values of log-transformed spectra in this wavelength range and their changes (denoted as $S_{350–400}$ and $\mathrm{DS}_{350–400}$, respectively) were used to quantify the binding of Zn^{2+}–SRFA.

The slope changes of log-transformed spectra in 350–400 nm ($\mathrm{DS}_{350–400}$) calculated for Zn^{2+}–SRFA at pH values ranging from 5.0 to 9.0 and an ionic strength at 0.01 mol L^{-1} are shown in Fig. 2.

The datasets of $\mathrm{DS}_{350–400}$ values in comparison with the concentrations of Zn^{2+}–SRFA complexes estimated using the NICA–Donnan model are shown in Fig. 3. These calculations used the complexation constants from Visual MINTEQ database (Supporting Information Table S1). For all examined pHs, $\mathrm{DS}_{350–400}$ values were linearly correlated with the modeled concentrations of SRFA-bound Zn^{2+}.

The competitive binding of Zn^{2+} and Ca^{2+} by SRFA was examined at pH 6.0. Background Ca^{2+} concentrations were set at 0.0, 0.00025 and 0.0025 mol L^{-1}, respectively. Differential spectra for this system were calculated and compared with the reference conditions with the same pH, ionic strength and the selected background Ca^{2+} concentration in the absence of Zn^{2+}. The differential spectra of the Ca^{2+}–Zn^{2+}–SRFA system for the three Ca^{2+} background levels and various total Zn^{2+} concentrations are shown in Fig. 4.

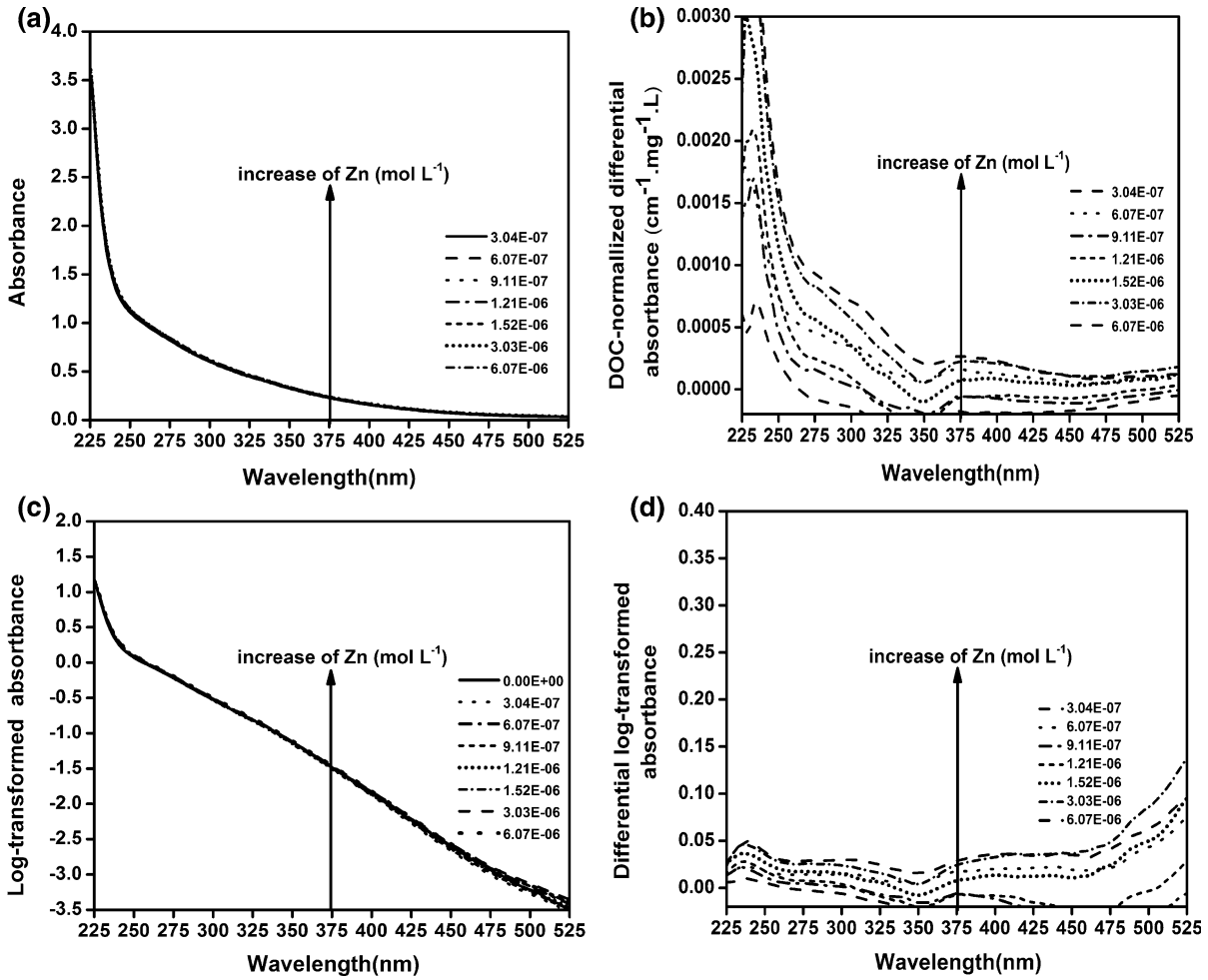

Fig. 1 Absorbance spectra of SRFA recorded at various concentrations of zinc at pH 9.0 and ionic strength 0.01 mol L^{-1}. **a** Zero-order spectra; **b** DOC-normalized differential spectra; **c** log-transformed spectra; and **d** differential log-transformed spectra at a constant DOC concentration 5.0 mg L^{-1} with cell length 5 cm and ref. without zinc

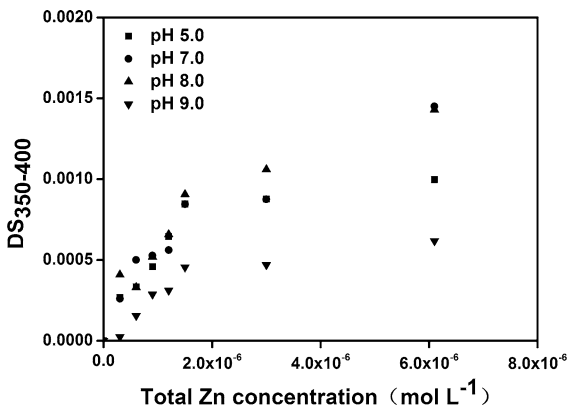

Fig. 2 Slope changes ($DS_{350–400}$) of the differential spectral as a function of Zn^{2+} concentrations at variations of pH at a constant ionic strength 0.01 mol L^{-1}

No obvious change in the shape of the Zn^{2+}-differential spectra was observed at various Ca^{2+} levels and the intensity of Zn^{2+}-differential spectra decreased in the presence of Ca^{2+}, which were similar to previous study (Gao et al. 2015a, b). This indicates that competing Ca^{2+} reduced the amount of SRFA sites available for Zn^{2+} binding. When comparing the intensity data of Zn^{2+}-differential spectra for different background concentrations of Ca^{2+}, the conspicuous site of the Zn^{2+}–SRFA absorbance with 0.00025 mol L^{-1} Ca^{2+} was different from others. A hypothesis was made that low Ca^{2+} concentration would be more influential. Further researches were needed here.

Similar results of SRFA spectra in the increasing concentration of Zn^{2+} and Ca^{2+} are shown in Fig. S2,

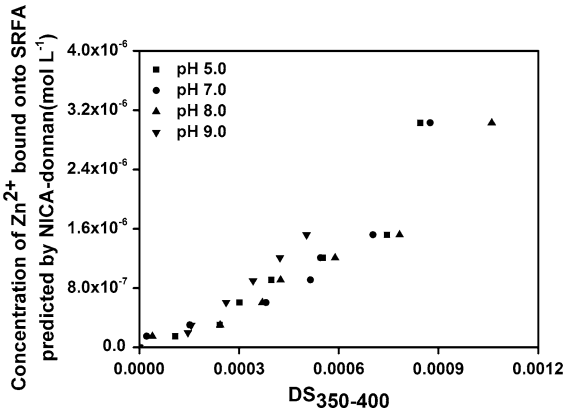

Fig. 3 Correlation between $DS_{350–400}$ and the amount of SRFA-bound Zn^{2+} predicted by using the NICA-Donnan model for variations of pH at ionic strength 0.01 mol L^{-1}

which proved that the slope of log-transformed absorbance of Zn^{2+}–Ca^{2+}–SRFA in the wavelengths range of 350–400 nm is most sensitive. The $DS_{350–400}$ was calculated at varying total zinc concentrations in three background levels of Ca^{2+} to illuminate the occurrence and contributions of these alternative mechanisms, as shown in Fig. 5.

This figure shows that $DS_{350–400}$ increases gradually with total Zn^{2+} concentrations, but this effect is suppressed by background Ca^{2+}.

The relationships between the changes of the spectral slope in the range of 350–400 nm and the Zn^{2+} concentrations bound to SRFA, simulated by the NICA–Donnan model, at three different Ca^{2+} concentrations, are shown in Fig. 6. These calculations

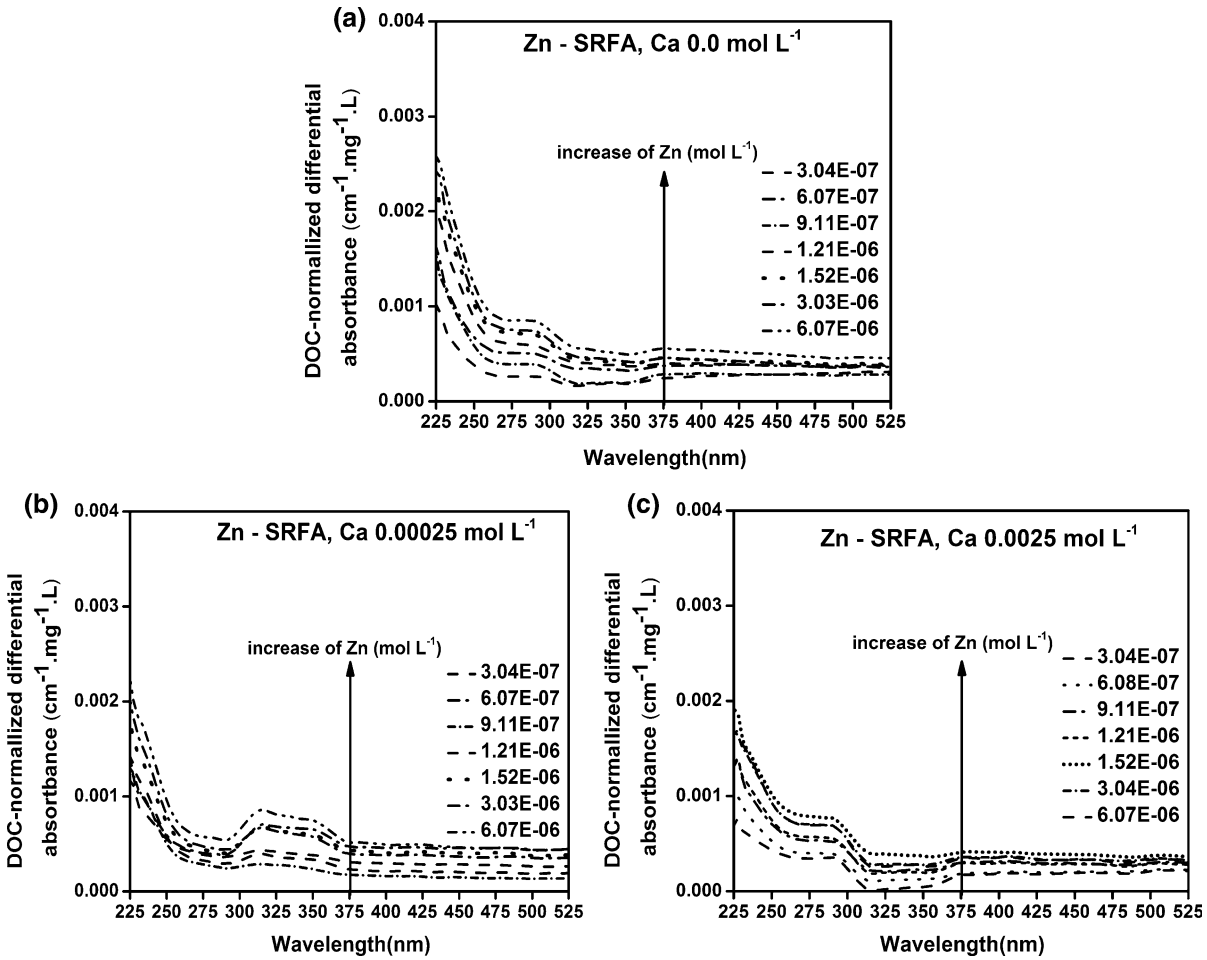

Fig. 4 Differential spectra of SRFA generated at various total concentrations of Zn^{2+}, with background Ca^{2+} concentration at: **a** 0 mol L^{-1}; **b** 0.00025 mol L^{-1}; and **c** 0.0025 mol L^{-1}, respectively, at a constant pH 6.0, ionic strength 0.01 mol L^{-1} and DOC 5.0 mg L^{-1}

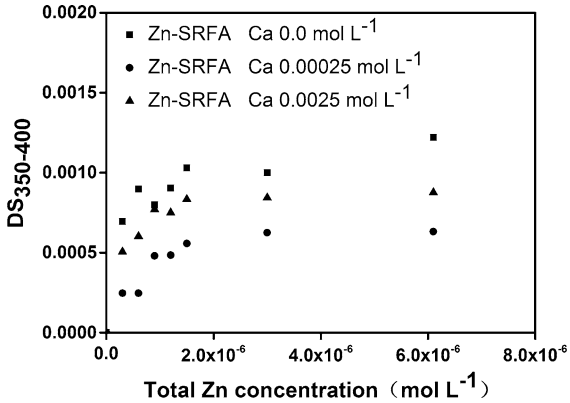

Fig. 5 Correlation between changes of the spectral slope in the range of 350–400 nm and total Zn^{2+} concentrations, at various background Ca^{2+} concentrations at a constant pH 6.0 and ionic strength 0.01 mol L^{-1}

used the complexation constants from Visual MINTEQ database (Supporting Information Table S1).

Correlation between $DS_{350–400}$ and the amount of SRFA-bound Zn^{2+} is predicted by the NICA–Donnan model for three different background Ca^{2+} levels at pH 6.0 and ionic strength 0.01 mol L^{-1}.

It demonstrates that for all examined background Ca^{2+} levels, $DS_{350–400}$ values measured in a wide range of Zn^{2+} concentrations are linearly correlated with the modeled concentrations of SRFA-bound Zn^{2+} irrespective of the background Ca^{2+} concentrations. Additionally, this figure also demonstrates that the $DS_{350–400}$ values did not form a simple dataset when compared with the sum of molar concentrations

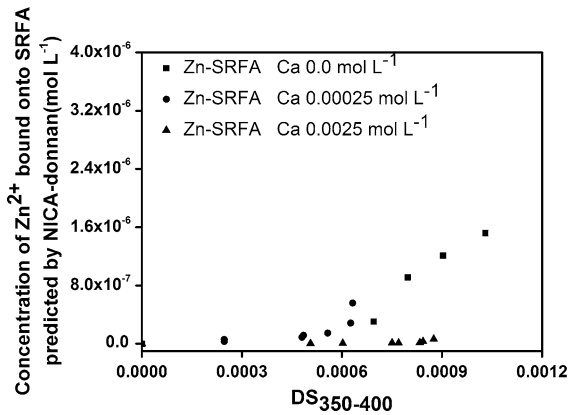

Fig. 6 Correlation between $DS_{350–400}$ and the amount of SRFA-bound Zn^{2+} predicted by using the NICA-Donnan model for various background Ca^{2+} concentrations at a constant pH 6.0 and ionic strength 0.01 mol L^{-1}

of Zn^{2+}–SRFA and Ca^{2+}–SRFA complexes ([Zn^{2+}–SRFA] + [Ca^{2}–SRFA]) in solutions, rather than α[Zn^{2+}–SRFA] +β [Ca^{2+}–SRFA] (α, β represent the account of the respective differential spectra).

Effect of Mg^{2+} on Zn^{2}–SRFA interaction

The competitive binding of Zn^{2+} and Mg^{2+} by SRFA was examined at the same condition as in Ca^{2+}–Zn^{2+}–SRFA systems except background Mg^{2+} levels at 0.0004 and 0.004 mol L^{-1}. Differential spectra for this system were calculated versus the reference conditions at the same pH, same ionic strength, no Zn^{2+}, and either selected background Mg^{2+} concentration. The differential spectra of Mg^{2+}–Zn^{2+}–SRFA are shown in Fig. 7.

In comparison with the data in Fig. 4a, the intensity of Zn^{2+}-differential spectra in the presence of Mg^{2+} was also suppressed; however, the effect of Mg^{2+} on the spectral intensity of Zn^{2+}–SRFA was less than Ca^{2+}. This indicates that Mg^{2+} would also compete with binding sites available for Zn^{2+}, the nature of these sites remained the same irrespective of the

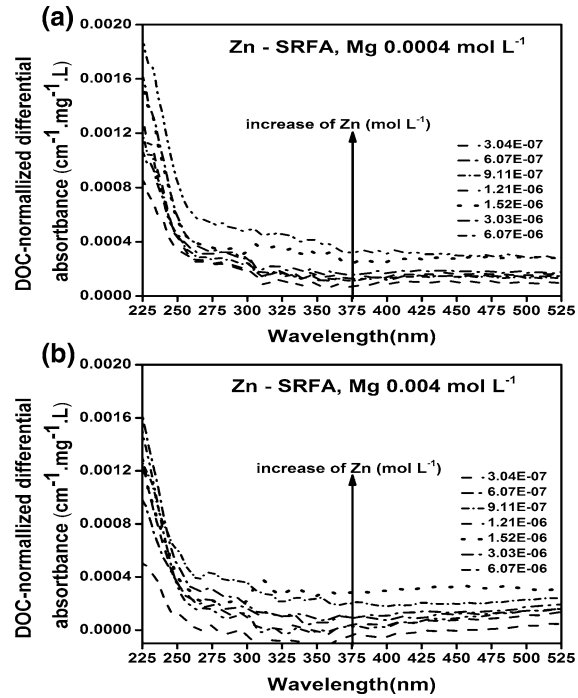

Fig. 7 Comparison of differential spectra of SRFA generated at different total concentrations of Mg^{2+}: **a** 0.0004 mol L^{-1}; **b** 0.004 mol L^{-1}, respectively, at a constant pH 6.0, ionic strength 0.01 mol L^{-1} and DOC 5.0 mg L^{-1}

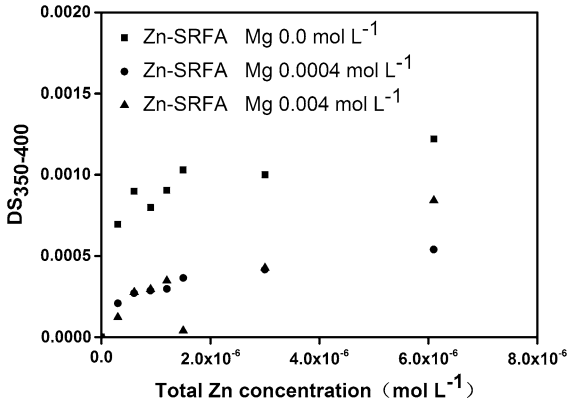

Fig. 8 Correlation between changes of the spectral slope in the range of 350–400 nm and total Zn^{2+} concentrations at different background magnesium levels at a constant pH 6.0 and ionic strength 0.01 mol L^{-1}

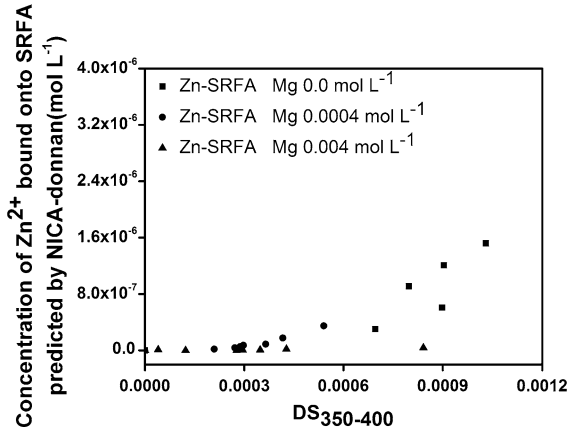

Fig. 9 Correlation between $DS_{350–400}$ and the amount of SRFA-bound Zn^{2+} predicted by the NICA–Donnan model for different background magnesium levels at a constant pH 6.0 and ionic strength 0.01 mol L^{-1}

background Mg^{2+} concentrations, but differential spectra of Zn^{2+}–SRFA have few obvious features in the presence of Mg^{2+}. The $DS_{350–400}$ of Zn^{2+}–Mg^{2+}–SRFA at various Zn^{2+} concentrations and different Mg^{2+} concentration is displayed in Fig. 8.

This figure evidences that $DS_{350–400}$ increases gradually with total Zn^{2+} concentrations in the presence of various Mg^{2+}, and the effect was suppressed similarly by 0.0004 mol L^{-1} Mg^{2+} or 0.004 mol L^{-1} Mg^{2}.

The relationships between $DS_{350–400}$ and concentrations of Zn^{2+} bound onto SRFA from the NICA–Donnan model in the presence of Mg^{2+} are shown in Fig. 9.

It manifests that $DS_{350–400}$ values in a wide range of Zn^{2+} concentrations are linearly correlated with the predicted Zn^{2+} concentrations, bound onto SRFA, irrespective of the background Mg^{2+} concentrations. Additionally, the $DS_{350–400}$ values are formed by datasets compared with the sum of molar concentrations of $\alpha[Zn^{2+}–SRFA] + \beta\ [Mg^{2+}–SRFA]$ (α, β represent the account of the respective differential spectra).

Conclusions

The differential spectra of Zn^{2+}–SRFA had consistent changes and performed metal-specific features, which reflected the nature and amount of interactions between Zn^{2+} and SRFA. The features in differential spectra were ascribed to carboxylic and phenolic functional groups in SRFA and caused by the replacement of the SRFA-bound protons by Zn^{2+}.

The differences in the effects of Zn^{2+} and Ca^{2+}/Mg^{2+} on SRFA chromophores allowed quantitating the competition between Zn^{2+} and Ca^{2+}/Mg^{2+} binding on SRFA sites in Zn^{2+}–Ca^{2+}/Mg^{2+}–SRFA system, which could be explained well by examining the intensity and shapes of differential spectra of SRFA. The features of differential spectra of Zn^{2+}–Mg^{2+}–SRFA system are not obvious. However, significant differences of the response were observed in Zn^{2+} differential spectra in the presence of 0.00025 mol L^{-1} Ca^{2+}, which require further investigation.

The binding of Zn^{2+} onto SRFA is not significantly affected by Mg^{2+} (e.g., 0.0005 or 0.005 mol L^{-1}) at pH 6.0. The competition of Zn^{2+}/Ca^{2+}/Mg^{2+} binding by SRFA can be quantified by calculating the $DS_{350–400}$ and predicted by the NICA–Donnan model. This study demonstrated the applicability of the NICA–Donnan model in elucidating interactions of the SRFA with Zn^{2+} at a wide range of pHs, and different concentrations of Ca^{2+} and Mg^{2+} by in situ absorbance. NICA–Donnan model can be used to gain further information about Me^{n+}–DOM interactions in the presence of various metals at different pHs and ionic strengths

Acknowledgements The authors acknowledge financial support from the Shenzhen Science and Technology Program (Grant JCYJ20160308103848156).

References

And, A. K., & Rorabacher, D. B. (1999). Noncomplexing tertiary amines as "better" buffers covering the range of pH 3–11. Temperature dependence of their acid dissociation constants. *Analytical Chemistry, 71*(15), 3140–3144.

Benedetti, M. F., Riemsdijk, W. H. V., Koopal, L. K., Kinniburgh, D. G., Gooddy, D. C., & Milne, C. J. (1996). Metal ion binding by natural organic matter: From the model to the field. *Geochimica et Cosmochimica Acta, 60*(14), 2503–2513.

Dryer, D. J., Korshin, G. V., & Fabbricino, M. (2008). In situ examination of the protonation behavior of fulvic acids using differential absorbance spectroscopy. *Environmental Science and Technology, 42*(17), 6644–6649.

Dudal, Y., & Gérard, F. (2004). Accounting for natural organic matter in aqueous chemical equilibrium models: A review of the theories and applications. *Earth-Science Reviews, 66*(3–4), 199–216.

Fortin, C., Couillard, Y., Vigneault, B., Vigneault, B., & Campbell, P. G. C. (2010). Determination of free Cd, Cu and Zn concentrations in lake waters by in situ diffusion followed by column equilibration ion-exchange. *Aquatic Geochemistry, 16*(16), 151–172.

Gao, Y. (2015). Effects of dissolved organic matter (DOM) on metal release from solid phases typical for corrosion processes and characterization of interactions between DOM and metal cations by in situ spectroscopic methods. ProQuest Dissertations & Theses, Ann Arbor, MI, USA, pp. 129.

Gao, Y., Yan, M. Q., & Korshin, G. V. (2015a). Effects of calcium on the chromophores of dissolved organic matter and their interactions with copper. *Water Research, 81,* 47–53.

Gao, Y., Yan, M. Q., & Korshin, G. V. (2015b). Effects of ionic strength on the chromophores of dissolved organic matter. *Environmental Science and Technology, 49*(10), 5905–5912.

Heijerick, D. G., & Janssen, C. R. (2000). Influence of water quality characteristics on the bioavailability and toxicity of zinc for three freshwater invertebrates. *Comparative Biochemistry and Physiology Part A: Molecular & Integrative Physiology, 126*(Suppl 1), 67.

Jones, A. M., Xue, Y., Kinsela, A. S., Wilcken, K. M., & Collins, R. N. (2016). Donnan membrane speciation of Al, Fe, trace metals and REEs in coastal lowland acid sulfate soil-impacted drainage waters. *Science of the Total Environment, 547,* 104–113.

Kinniburgh, D. G., Riemsdijk, W. H. V., Koopal, L. K., Borkovec, M., Benedetti, M. F., & Avena, M. J. (1999). Ion binding to natural organic matter: Competition, heterogeneity, stoichiometry and thermodynamic consistency. *Colloids and Surfaces A: Physicochemical and Engineering Aspects, 151*(1), 147–166.

Kuhn, K. M., Neubauer, E., Hofmann, T., Von Der, K. F., Aiken, G. R., & Maurice, P. A. (2015). Concentrations and distributions of metals associated with dissolved organic matter from the Suwannee River. *Environmental Engineering Science, 32,* 54–65.

Leenheer, J. A., & Croué, J. P. (2003). Characterizing aquatic dissolved organic matter. *Environmental Science and Technology, 37*(1), 18A–26A.

Maurice, P. A. (2015). Special issue introduction: Dissolved organic matter from the Suwannee River (GA, USA). *Environmental Engineering Science, 32*(1), 1–3.

Milne, C. J., Kinniburgh, D. G., van Riemsdijk, W. H., & Tipping, E. (2003). Generic NICA-Donnan model parameters for metal-ion binding by humic substances. *Environmental Science and Technology, 37*(5), 958–971.

Mueller, K. K., Lofts, S., Fortin, C., & Campbell, Peter G. C. (2012). Trace metal speciation predictions in natural aquatic systems: incorporation of dissolved organic matter (DOM) spectroscopic quality. *Environmental Chemistry, 9*(4), 356–368.

Schamphelaere, K. A. C. D., Unamuno, V. I. R., Tack, F. M. G., Vanderdeelen, J., & Janssen, C. R. (2005). Reverse osmosis sampling does not affect the protective effect of dissolved organic matter on copper and zinc toxicity to freshwater organisms. *Chemosphere, 58*(5), 653–658.

Valilue, Z., Vardin, M. T., & Kalhor, E. G. (2016). Design and construction of ion-selective electrode based on a new Schiff base and its application in determination of copper (II) ions. *Indian Journal of Chemistry Section A-Inorganic Bio-Inorganic Physical Theoretical & Analytical Chemistry, 55*(1), 51–56.

Waşąg, J., & Grabarczyk, M. (2016). Adsorptive stripping voltammetry of In (III)) in the presence of cupferron using an in situ plated bismuth film electrode. *Analytical Methods, 8*(17), 3605–3612.

Yan, M. Q., & Korshin, G. V. (2004). Comparative examination of effects of binding of different metals on chromophores of dissolved organic matter. *Environmental Science and Technology, 48,* 3177–3185.

Yan, M. Q., Lu, Y. J., Gao, Y., Benedetti, M. F., & Korshin, G. V. (2015). In-situ investigation of interactions between magnesium ion and natural organic matter. *Environmental Science and Technology, 49*(14), 8323–8329.

Yan, M. Q., Ma, J., & Ji, G. (2016). Examination of effects of Cu(II) and Cr(III) on Al(III) binding by dissolved organic matter using absorbance spectroscopy. *Water Research, 93,* 84–90.

Yan, M. Q., Wang, D., Korshin, G. V., & Benedetti, M. F. (2013). Quantifying metal ions binding onto dissolved organic matter using log-transformed absorbance spectra. *Water Research, 47*(7), 2603–2611.